COSMIC AND SUBATOMIC PHYSICS REPORT
LUIP 9301
JANUARY 1993
ISRN LUNFD6/NFFK—7137—SE+25P
ISSN 0348-9329

ON THE JET-LIKE AND RING-LIKE SUBSTRUCTURE IN DISTRIBUTIONS OF PRODUCED PARTICLES IN CENTRAL HEAVY-ION COLLISIONS AT ULTRA-RELATIVISTIC ENERGIES

(EMU01-collaboration)

M I Adamovich[13], M M Aggarwal[4], Y A Alexandrov[13], N P Andreeva[1], Z V Anzon[1], R Arora[4], F A Avetyan[20], S K Badyal[8], E Basova[17], K B Bhalla[7], A Bhasin[8], V S Bhatia[4], V G Bogdanov[15], V I Bubnov[1], T H Burnett[16], X Cai[18], I Y Chasnikov[1], L P Chernova[18], M M Chernyavsky[13], G Z Eligbaeva[1], L E Eremenko[1], A S Gaitinov[1], E R Ganssauge[12], S Garpman[11], S G Gerassimov[13], J Grote[16], K G Gulamov[18], S K Gupta[7], V K Gupta[8], H H Heckman[3], H Huang[19], B Jakobsson[11], B Judek[14], L Just[9], S Kachroo[8], G S Kalyachkina[1], E K Kanygina[1], M Karabova[6,9], G L Kaul[8], S Kitroo[8], S P Kharlamov[13], S A Krasnov[6], S Kulikova[6], V Kumar[7], P Lal[7], V G Larionova[13], V N Lepetan[1], L S Liu[18], S Lokanathan[7], J Lord[16], N S Lukicheva[18], S B Luo[10], T N Maksimkina[6], L K Mangotra[8], N A Marutyan[20], N V Maslennikova[13], I S Mittra[4], S Mookerjee[7], H Nasrulaeva[17], S H Nasyrov[17], V S Navotny[18], J Nystrand[11], G I Orlova[13], I Otterlund[11], H S Palsania[7], N G Peresadko[13], N V Petrov[17], V A Plyushchev[15], D A Qarshiev[17], W Y Qian[19], Y M Qin[10], R Raniwala[7], S Raniwala[7], N K Rao[8], V M Rappoport[13], J T Rhee[12], N Saidkhanov[18], N A Salmanova[13], L G Sarkisova[20], V R Sarkisyan[20], G S Shabratova[6], T I Shakhova[1], S N Shpilev[18], D Skelding[16], K Söderström[11], Z I Solovjeva[15], E Stenlund[11], E L Surin[18], L N Svechnikova[18], K D Tolstov[6], M Tothova[9], M I Tretyakova[13], T P Trofimova[17], U Tuleeva[17], S Vokal[6,9], H Q Wang[19], Z Q Weng[5], R J Wilkes[16], Y L Xia[5], G F Xu[2], D H Zhang[10], P Y Zheng[2], S I Zhokhova[18] and D C Zhou[19]

1) Alma Ata, Inst. of High Energy Physics, Kazakhstan
2) Beijing, Academica Sinica, People's Republic of China
3) Berkeley, Lawrence Berkeley Lab, USA
4) Chandigarh, Panjab University, India
5) Changsa, Hunan Education Institute, People's Republic of China
6) Dubna, JINR, Russia
7) Jaipur, University of Rajasthan, India
8) Jammu, University of Jammu, India
9) Kosice, Safarik University, Czechoslovakia
10) Linfen, Shanxi Normal University, People's Republic of China
11) Lund, University of Lund, Sweden
12) Marburg, Philipps University, Germany
13) Moscow, Lebedev Institute, Russia
14) Ottawa, NRC, Canada
15) St Petersburg, V G Khlopin Radium Institute, Russia
16) Seattle, University of Washington, USA
17) Tashkent, Institute of Nuclear Physics, Uzbekistan
18) Tashkent, Physical-Technical Institute, Uzbekistan
19) Wuhan, Hua-Zhong Normal University, People's Republic of China
20) Yerevan, Physical Institute, Armenia

ABSTRACT

The azimuthal substructure of particles produced in ultra-relativistic heavy-ion collisions is investigated. The observed substructure seems to be of stochastic nature and the features of the experimental data can be understood when effects like γ-conversion and particle interference (HBT) are taken into account.

1 Introduction

Whenever densities of secondary particles produced in high energy interactions between particles of various kinds are analysed in terms of fluctuations, the observed effects are dominated by statistical fluctuations. Significant deviations from these statistical fluctuations are only observed after painstaking efforts to remove the statistical part of the fluctuations. Several such attempts have been made during recent years[1] most of which have utilized variations of the method with factorial moments proposed by Bialas and Peschanski[2].

At the same time, when individual events are imaged visually, the human eye, however, has a tendency to observe all kinds of intricate patterns. For instance, when azimuthal distributions of particles from relativistic heavy ion collisions, produced within a narrow region of pseudo-rapidity, are studied, the eye spontaneously suggests a classification into two classes; distributions with a jet-like structure and distributions with a ring-like structure. These structures are also referred to as tower and wall structures[3]. The jet-class consists of cases where several particles seem to form clusters in the azimuthal plane, clusters which are separated with rather large void regions, as sketched in fig. 1a. The ring-class consists of cases where the particles are distributed almost regularly as the spokes in a wheel (cf. fig. 1b).

When a factorial moment analysis is performed in one (e.g. pseudorapidity, η) and two dimensions (e.g. pseudorapidity and azimuth) the same two classes emerge[4]. In a one-dimensional analysis the main contributions come from ring-like substructures in the event whereas in a two-dimensional analysis jet-like substructures are the dominant contributors.

In this paper we have made an attempt to see if two such classes, jet-like and ring-like, have any physical significance in the particle production in high energy heavy ion interactions, or if they are of purely stochastic nature. For this purpose we apply a new method which will be described in section 3 and the results of the analysis will be given in section 4.

2 The Experiment

The EMU01-collaboration has collected data from collisions between various projectiles and targets at different incident energies in the ultra-relativistic

region[5]. Two different techniques have been employed, both utilizing nuclear emulsion; ordinary emulsion stacks with exposures parallel to the emulsion plates and emulsion chambers in which the exposures are perpendicular to the plates. The second technique is best suited for an analysis in which the azimuthal emission angles are of interest since, in this case, the detector has azimuthal symmetry and high resolution. With this technique a resolution of $\Delta\eta \approx 0.013$ rapidity units in the central region can be obtained[6]. Pseudorapidity is given by $\eta = -\ln(\mathrm{tg}(\theta/2))$, where θ is the emission angle with respect to the beam direction. A major fraction of the chambers are equipped with thin target foils, providing possibilities to study interactions with various targets.

In this paper we have analyzed data from interactions induced by the CERN/SPS 200 A GeV oxygen and sulfur beams on targets of emulsion, silver and gold recorded in emulsion chambers.

Further details on the experiment, measurements and experimental criteria can be found elswhere[7].

3 The Method

Many different ways of sampling narrow, dense groups of particles can be devised. One method is to use a fixed scale of length $\Delta\eta_d$, and to move it continuously along the rapidity axis. Each group will then be described by a multiplicity n_c and a density $\rho_c = n_c/\Delta\eta_d$. All groups where $\rho_c > (\rho_c)_{cut}$ can then be recorded and used in the subsequent analysis. This method has the drawback that the sample will consist of several different multiplicities n_c, which will make the study of the azimuthal structures unnecessarily complicated. Furthermore the discarded groups with $\rho_c < (\rho_c)_{cut}$ will have yet other multiplicities, preventing a direct comparison between the dense and the more dilute groups.

Another method, in contrast to the previous one, is to keep the multiplicity n_d fixed. Each consecutive n_d-tuple of particles along the η-axis can then be considered as a group characterized by $\Delta\eta_c$ and $\rho_c = n_d/\Delta\eta_c$. Dense groups can then be defined and recorded as above. This method has the advantage that all groups, including the discarded, more dilute ones, have by definition the same multiplicity n_d, and can be readily compared. With this method it is also a fairly simple task to compare the obtained sample with samples obtained by a purely stochastic process as well as samples obtained from model-based

Monte-Carlo calculations.

Next we need to parameterize the azimuthal structure in a suitable way, so that large values of the parameter represent one type of structure and small values the other. Two sums have been suggested as such parameters[8] and are given by

$$S_1 = -\sum \ln(\Delta\phi_i) \tag{1}$$

and

$$S_2 = \sum (\Delta\phi_i)^2 \tag{2}$$

where $\Delta\phi$ is the azimuthal difference between two neighboring particles in the group. For the sake of simplicity we can count $\Delta\phi$ in units of full revolutions and thus we have

$$\sum (\Delta\phi_i) \equiv 1 \tag{3}$$

Both these parameters will be large ($S_1 \to \infty$, $S_2 \to 1$) for jet-like structures and small ($S_1 \to n_d \cdot \ln n_d$, $S_2 \to 1/n_d$) for ring-like structures. Furthermore the expectation values for the two parameters, in a purely stochastic scenario with independent particles, can be analytically expressed as

$$\langle S_1 \rangle = n_d \cdot \sum_{k=1}^{n_d-1} \frac{1}{k} \tag{4}$$

and

$$\langle S_2 \rangle = \frac{2}{n_d + 1} \tag{5}$$

respectively. Both these expectation values can be derived from the distribution of gaps between azimuthal neighbors given by

$$f(\Delta\phi)\, d(\Delta\phi) = (n_d - 1)\cdot(1 - \Delta\phi)^{(n_d - 2)} d(\Delta\phi) \tag{6}$$

Although the two parameters S_1 and S_2 have similar features S_1 is essentially only sensitive to the smallest gaps, $\Delta\phi$, whereas the main contribution to S_2 comes from the largest gaps or the voids in the group. In this respect the two parameters are complementary and in the next section both parameters will be

used. It should be noted that it is enough with one extremely small gap in order to obtain a large value of S_1. S_1 will thus be very sensitive to any kind of pair production of particles, e.g. electron-positron pairs from γ-conversion.

4 Results

Average values of the parameters S_1 and S_2 (eqs. 1 and 2) are calculated in the region $1.32 < \eta < 6.0$ as functions of the size of the group, $\Delta\eta = \eta_{max} - \eta_{min}$, where η_{min} and η_{max} are the pseudo-rapidity values of the first and last particles in the group. In fig. 2 we show the results for central 200 A GeV O+Ag(Br) collisions; fig. 2a for S_1, fig. 2b for S_2. A total multiplicity of at least 150 produced charged particles (shower particles) was required and n_d is chosen to 17. The dashed lines correspond to the stochastic averages given by eqs. 4 and 5. Since each consecutive n_d-tuple of particles along the η-axis is considered, a given particle may belong to several groups. In the error calculation this has to be taken into account, and furthermore it means that the data points are somewhat correlated. The sizes of the error bars have also been checked by use of Monte-Carlo methods. Also indicated in the figures are the outcome of the same analysis performed on a sample of collisions generated by FRITIOF 1.7[9]. As can be seen in figs. 2a and 2b there is good agreement between FRITIOF and stochastic averages, and this agreement is found also for other projectile-target combinations. The data points have a weak tendency to be above the stochastic averages indicated by the dashed line (i.e. towards jet-structure). Furthermore there seems to be no significant dependence on the group size, $\Delta\eta$. If n_d is varied the results are very similar.

In fig. 3 the results for the data set from 200 A GeV S+Ag collisions are given. Again the data points are somewhat above the stochastic level (and FRITIOF), but no significant $\Delta\eta$-dependence is seen.

In fig. 4 the analysis is repeated for 200 A GeV S+Au collisions. In this case the data is significantly above the stochastic level. This clearly indicates that a certain "jettyness" is present.

A comparison between the three data-sets thus reveals that the observed structure is on the jet-like side (above the stochastic level) and any sign of ring-like structure (below the stochastic level) is washed out in the averaging.

In an earlier analysis with 2-dimensional factorial moments[4] it was found that the background from γ-conversion in the S+Au sample, estimated to be 3 % of

all gammas (smaller for the other samples), to a large extent could explain the observed effects. We have thus also generated a FRITIOF-sample in which 3 % of the produced gammas are converted to electron-positron pairs according to the description of Borzelino[10]. The results from the analysis of this sample are also given in fig. 4. As can be seen in fig. 4a, there is a satisfactory agreement between the data and the sample from FRITIOF+γ-conversion when S_1 is used. However, the results in fig. 4b, where S_2 is used, clearly indicates that the global structure in the two samples differ considerably, especially for the rather dilute groups. We thus conclude that the small gap structure is a consequence of γ-conversion, but that the real sample shows larger void regions in than the generated sample.

Another effect, not accounted for by FRITIOF 1.7, which is of relevance here, is the Hunbury-Brown and Twiss effect (HBT), originating from the interference between identical particles. In order to study how the HBT effect would influence our results we have parameterized the effect and slightly shifted particles in a FRITIOF generated sample accordingly, in much the same way as the effect is mimiced in recent versions of JETSET[11]. Using a static Gaussian distribution model[12] with a source radius of 3.5 fm and a chaotisity parameter of 0.7, only considering pions, we obtain the correlation function $C_2(Q)$, given in fig. 5, where Q is the four-momentum difference between the two particles in the pair. As can be seen this essentially imitates the HBT-effect and enhances the probability for particles to end up with smaller relative space angles.

Fig. 6 shows the results of the analysis of the generated FRITIOF+HBT sample, with and without γ-conversion, compared with the results obtained from the data. From these results we can conclude that the HBT-effect qualitatively explains the general trend of the data, and an even better agreement would be possible to achieve with a tuning of the radius and chaotisity parameters. Except for some additional jet-structure seen by the S_2 parameter for the dilute groups, the features of the data can be understood as a superposition of stochastic fluctuations, γ-conversion and particle interference. This small excess cannot be accounted for even if the HBT-parameters are tuned, since that would mean that the jet-structure for the dense groups would be much more pronounced than in the data.

In fig. 7 we have compared the distribution of the structure parameters from individual dense groups (n_d = 35; $0.0 < \Delta\eta \leq 0.2$) obtained from the different S+Au samples; fig. 7a for S_1, fig. 7b for S_2. All the distributions have similar

shapes, although there is a weak tendency for the experimental distribution to be broader. There is however no signal for any separation between the two classes with jet-like and ring-like structures. Dilute groups show the same features. The ring-like tails (left side of the distributions) are nicely reproduced by stochastic emission, clearly indicating the origin of the ring-structure. In the right tails (jet-like region) there are deviations between the different distributions. Distributions for dilute groups ($0.5 < \Delta\eta < 1.0$) show the same features. Furthermore the features are independent of the chosen multiplicity n_d.

Figure 8a displayes experimental azimuthal distributions from a typical example of a group with large values of the parameters, i.e. corresponding to jet-structure, and fig 8b shows a typical example of a ring-structure found in the data (cf. fig 1). However in the analysis presented here such jet-like and ring-like events do not exhibit significant deviations from what can be expected from stochastic emission.

5 Conclusions

We have investigated the azimuthal substructure of particles from central high energy heavy ion collisions, produced within dense and dilute groups along the rapidity axis. The jet- and ring-like structures, suggested by studies of one- and many-dimensional factorial moments, seem to lack any physical significance, i.e. no large deviations from the stochastic averages are seen. The "jettyness" observed in the data can essentially be attributed to electron-positron pairs from γ- conversion and to particle interference between identical particles (HBT). However, when the parameter S_2 (eq. 2) is used in the analysis there seems to be some jet-structure for the dilute groups which cannot be accounted for, not even with a stronger interference effect.

Acknowledgements

The financial support from the Swedish Natural Science Research Council, the German Federal Minister of Research and Technology, The University Grants Commission, Government of India, The National Science Foundation of China, The Distinguished Teacher Foundation of the State Education Commission of China, The Fok Ying Tung Education and The US Department of Energy and National Science

Foundation are gratefully acknowledged.

References

[1] See, for instance, Proc Workshop on Multiparticle Production - Fluctuations and Fractal Structure, Ringberg Castle, Germany, June 25 - 28, 1991. (World Scientific, 1992).
[2] A Bialas and R Peschanski, Nucl Phys B273(1986)703; B308(1988)857.
[3] R Peschanski, communication at the XXII Int Symp on Multiparticle Dynamics, Santiago di Compostella, Spain, July 12-17, 1992.
[4] M I Adamovich et al (EMU01-collaboration), Lund University Preprint LUIP 9202 (Lund, 1992), submitted to Nucl Phys B.
[5] M I Adamovich et al (EMU01-collaboration), Phys Rev Lett 69(1992)745.
[6] S Garpman et al, Nucl Instr & Meth A269(1988)134.
[7] M I Adamovich et al (EMU01-collaboration), Phys Lett B223(1989)262; Phys Rev Lett 62(1989)2801.
[8] E Stenlund et al (EMU01-collaboration), Nucl Phys A498(1989)541c.
[9] B Nilsson-Almquist and E Stenlund, Comp Phys Comm 43(1987)387.
[10] A Borzelino, Phys Rev 89(1953)1023.
[11] T Sjöstrand, CERN Preprint CERN-TH.6488/92 (CERN May 1992).
[12] F B Yano and S E Koonin, Phys Lett B78(1978)556.

Figure captions

Figure 1: Examples of two extreme azimuthal structures.
a) Jet-like. b) Ring-like.

Figure 2: The dependence of the parameters a) $\langle S_1 \rangle$ and b) $\langle S_2 \rangle$ on group size, $\Delta\eta$, for central 200 A GeV O+Ag(Br) interactions. The dashed lines indicate the expectation values for purely stochastic emission. S1 and S2 are given by eqs. 1 and 2, respectively.

Figure 3: As fig. 2, but for S+Ag.

Figure 4: As fig. 2, but for S+Au.

Figure 5: The correlation function $C_2(Q)$ obtained by mimicing the interference between identical pions (HBT).

Figure 6: As fig. 4, but including the HBT-effect.

Figure 7: Probability distributions a) $P(S_1)$ and b) $P(S_2)$ for central S+Au interactions at 200 A GeV.

Figure 8: Examples of two extreme structures found in the experimental data.
a) Jet-like. b) Ring-like. The numbers indicate directions where there are several close particles.

The figures have been incorrectly numbered. The figure numbered 8 should be number 5 and the figures numbered 5-7 are consequently figures 6-8.

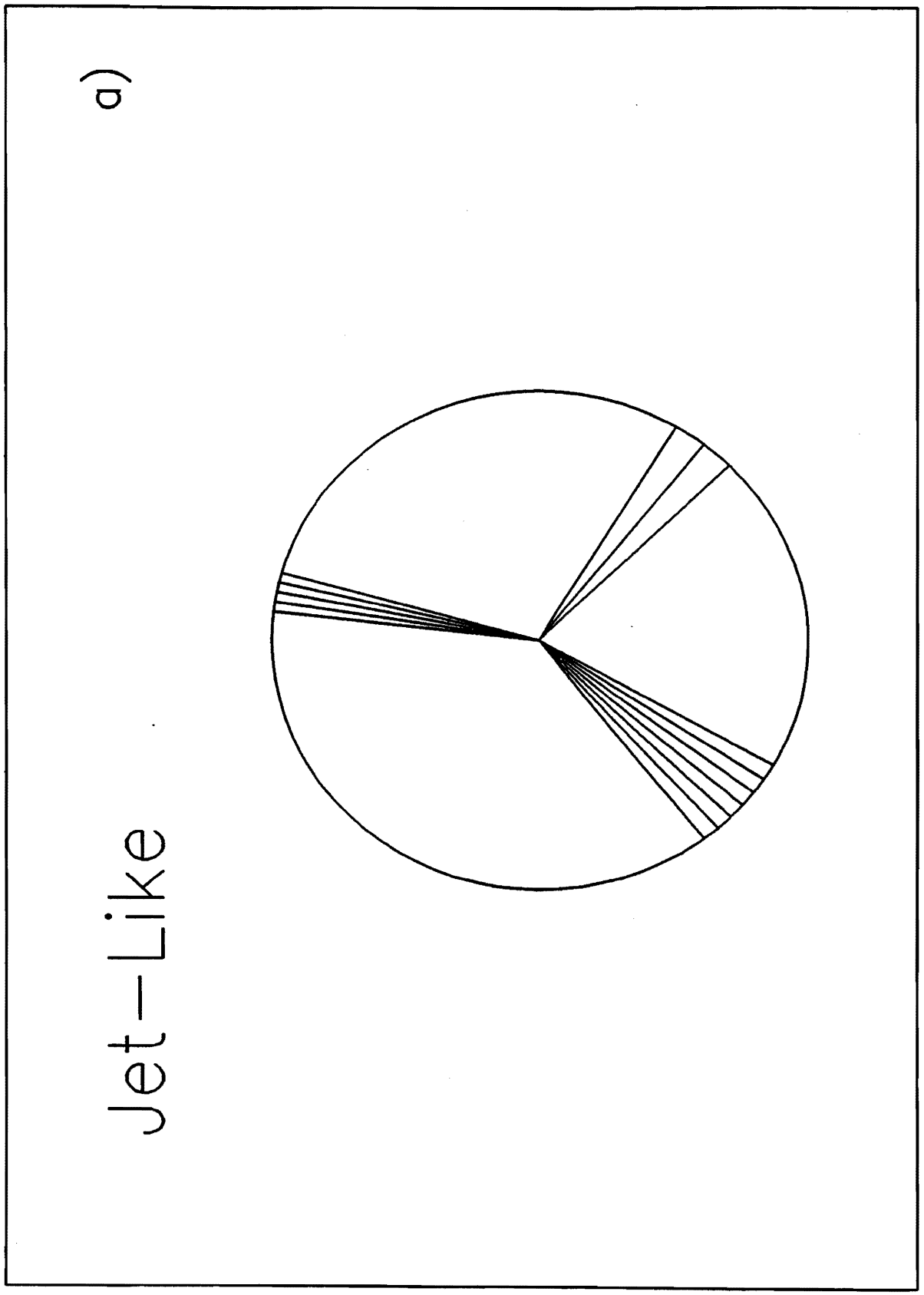

Fig. 1

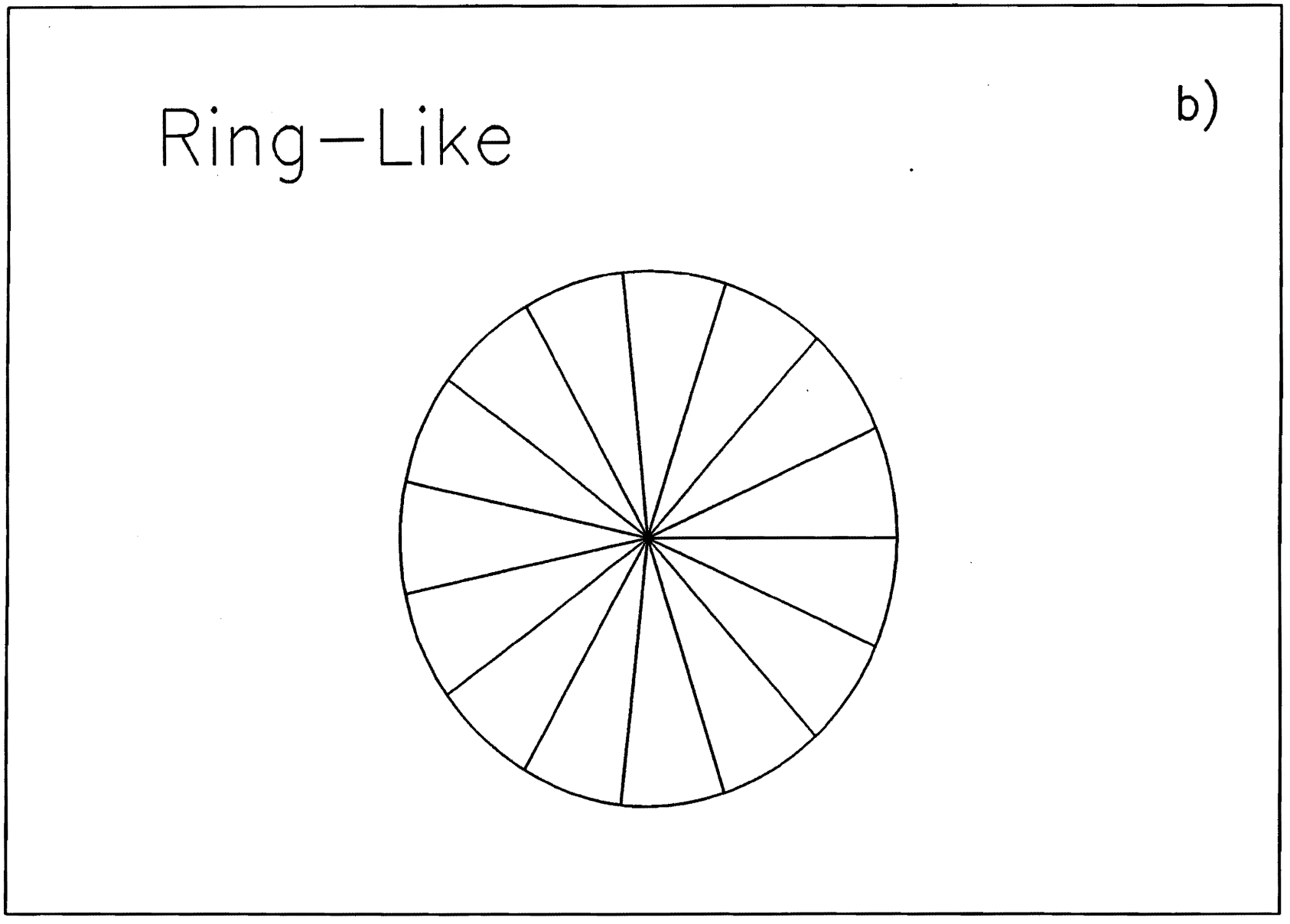

Fig. 1

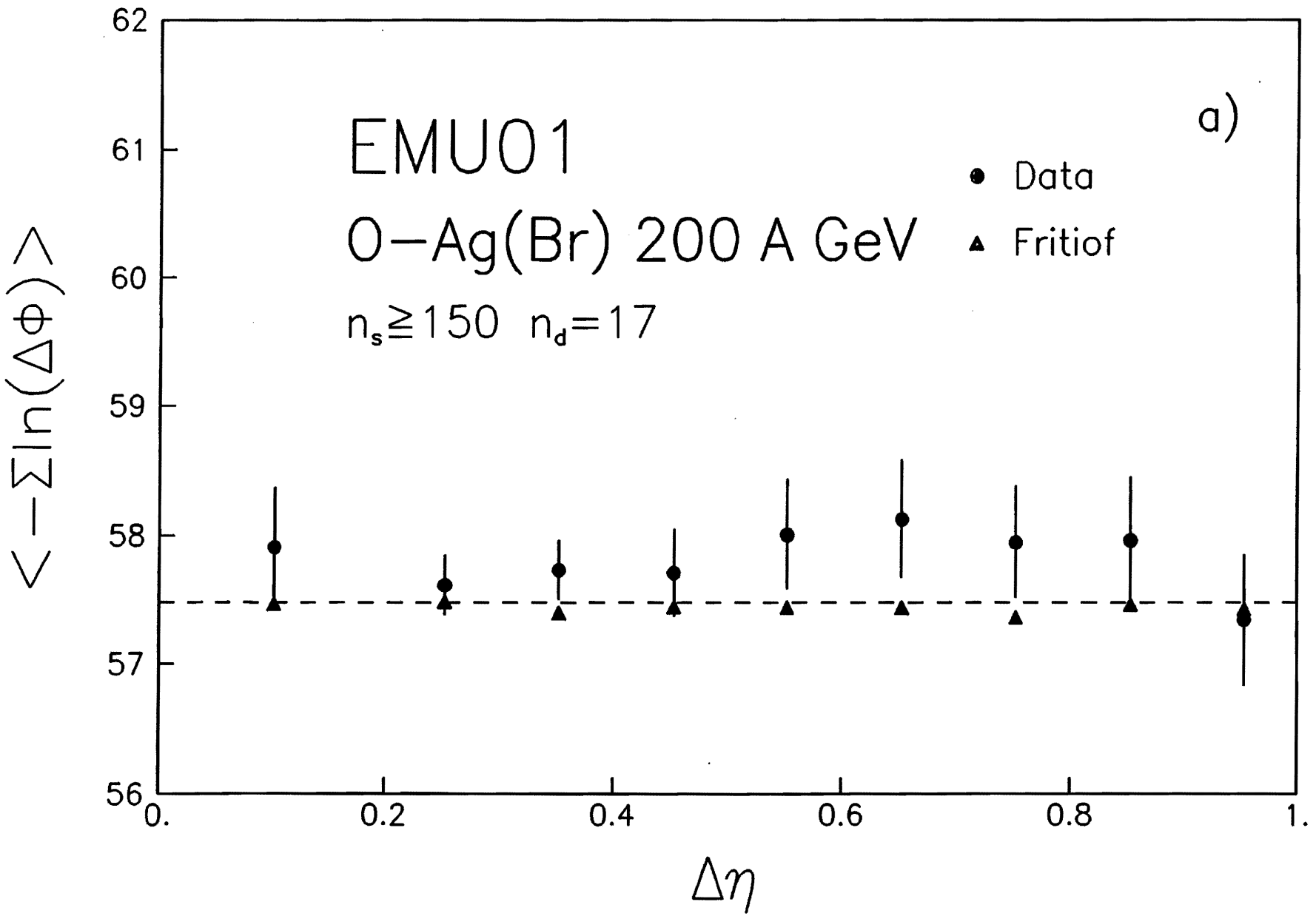
EMU01
O−Ag(Br) 200 A GeV
$n_s \geq 150$ $n_d = 17$
a)
Data
Fritiof
$< -\sum \ln(\Delta\phi) >$
$\Delta\eta$
62
61
60
59
58
57
56
0.
0.2
0.4
0.6
0.8
1.

Fig. 2

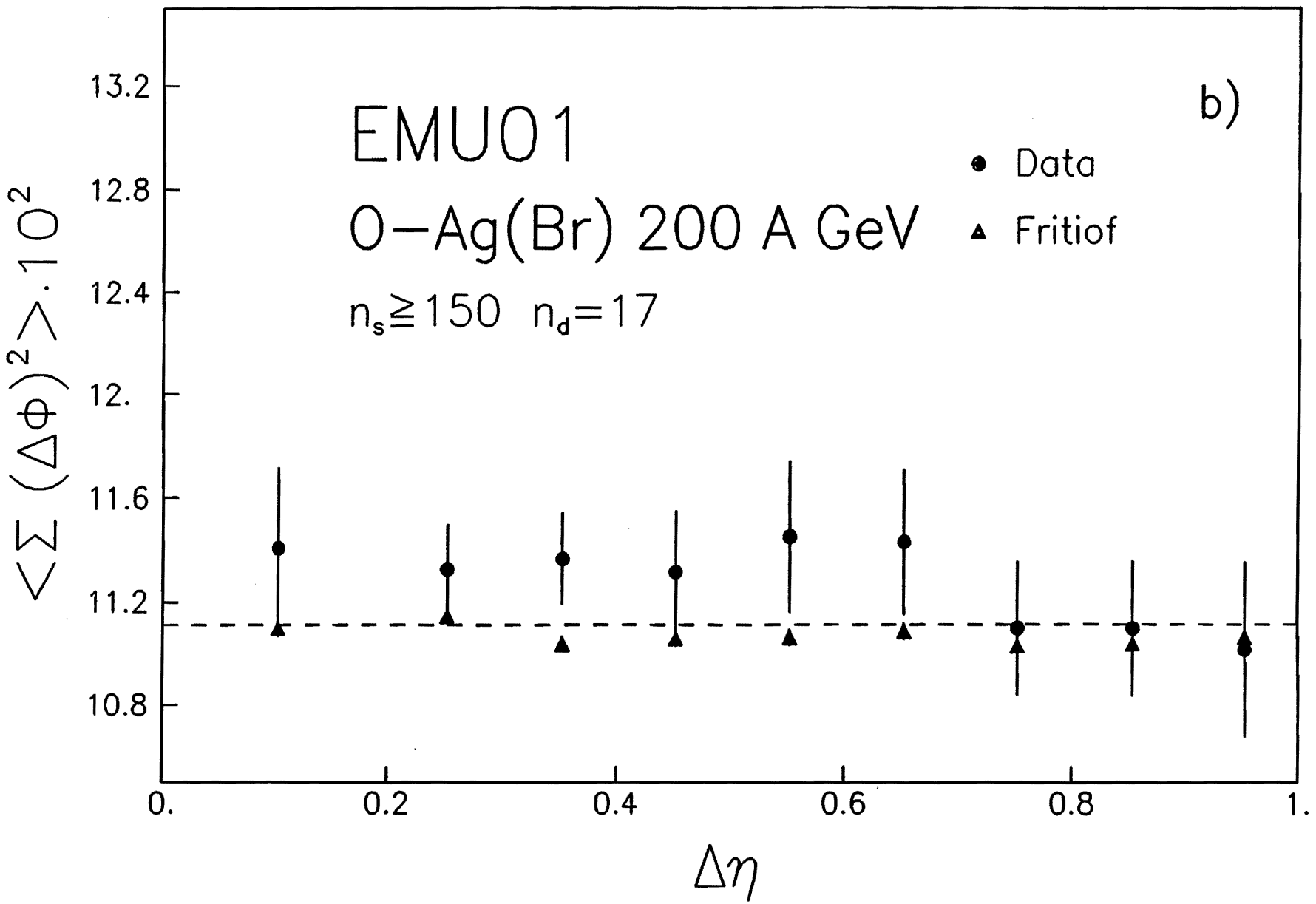
EMU01
O–Ag(Br) 200 A GeV
$n_s \geq 150$ $n_d = 17$
b)
Data
Fritiof
$\langle \sum (\Delta\phi)^2 \rangle \cdot 10^2$
13.2
12.8
12.4
12.
11.6
11.2
10.8
0.
0.2
0.4
0.6
0.8
1.
$\Delta\eta$

Fig. 2

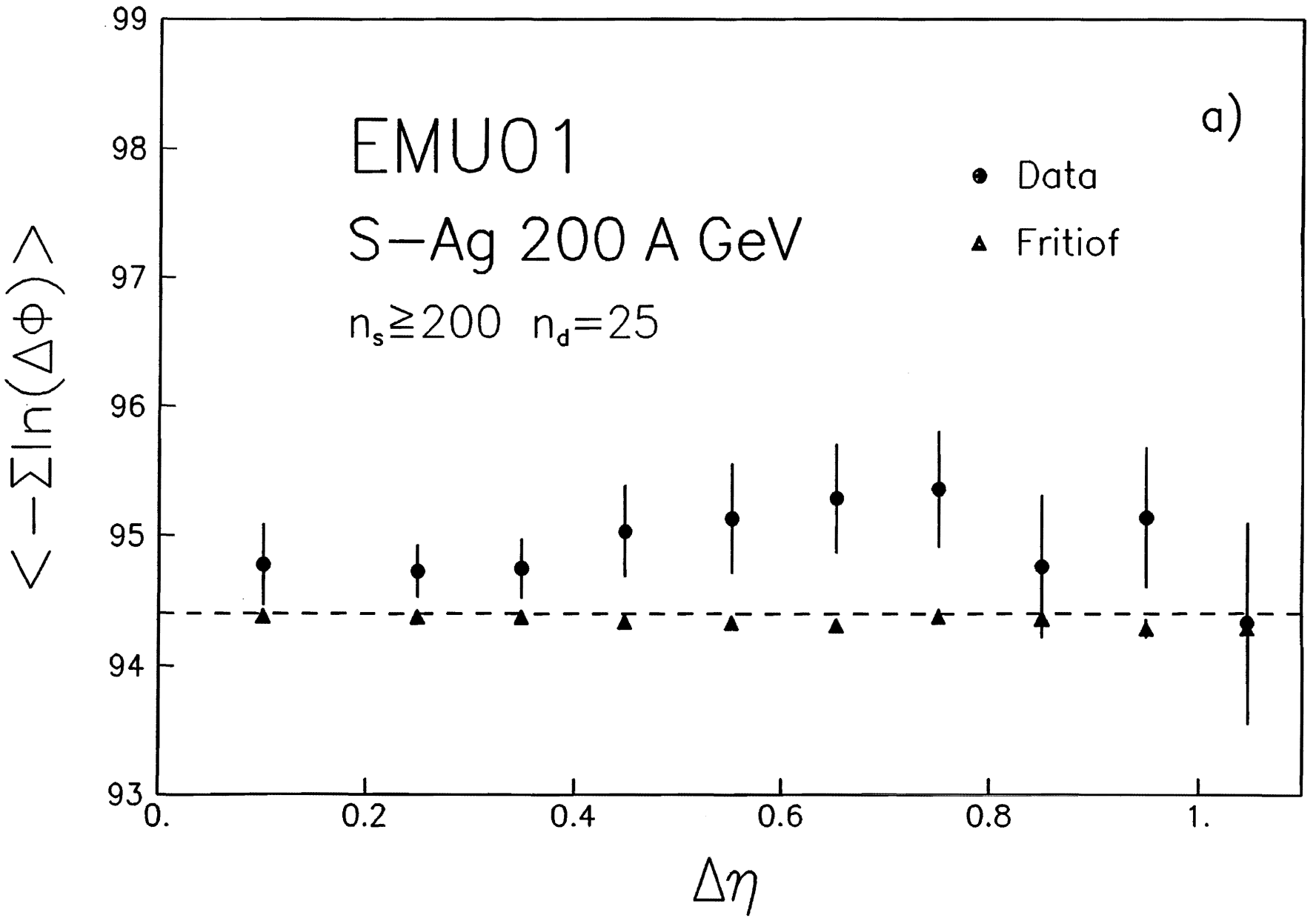
EMU01
S–Ag 200 A GeV
$n_s \geq 200$ $n_d = 25$
a)
Data
Fritiof
$< -\sum \ln(\Delta\phi) >$
$\Delta\eta$
99
98
97
96
95
94
93
0.
0.2
0.4
0.6
0.8
1.

Fig. 3

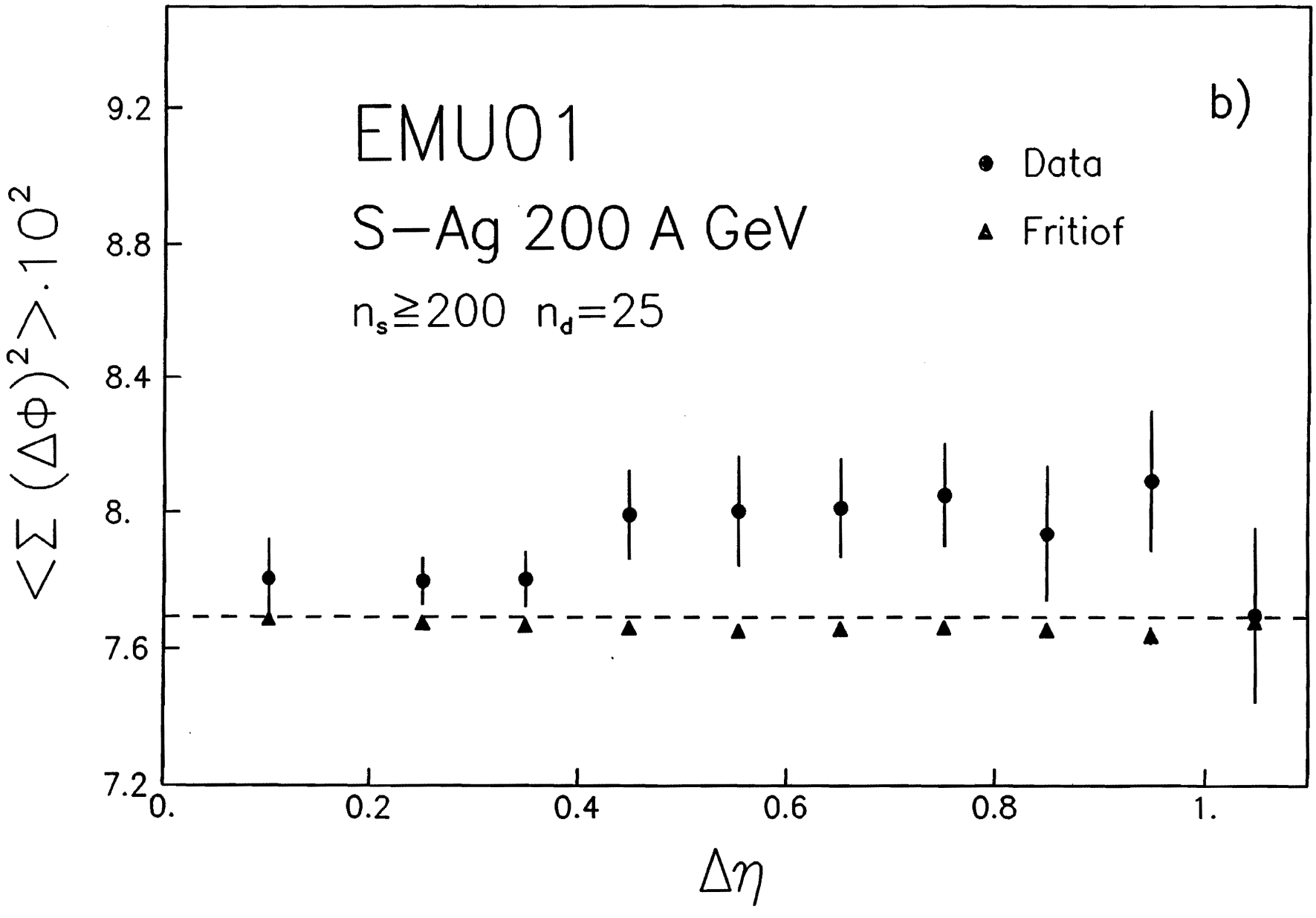
EMU01
S−Ag 200 A GeV
$n_s \geq 200$ $n_d = 25$
b)
Data
Fritiof
$\langle \sum (\Delta\phi)^2 \rangle \cdot 10^2$
9.2
8.8
8.4
8.
7.6
7.2
0.
0.2
0.4
0.6
0.8
1.
$\Delta\eta$

Fig. 3

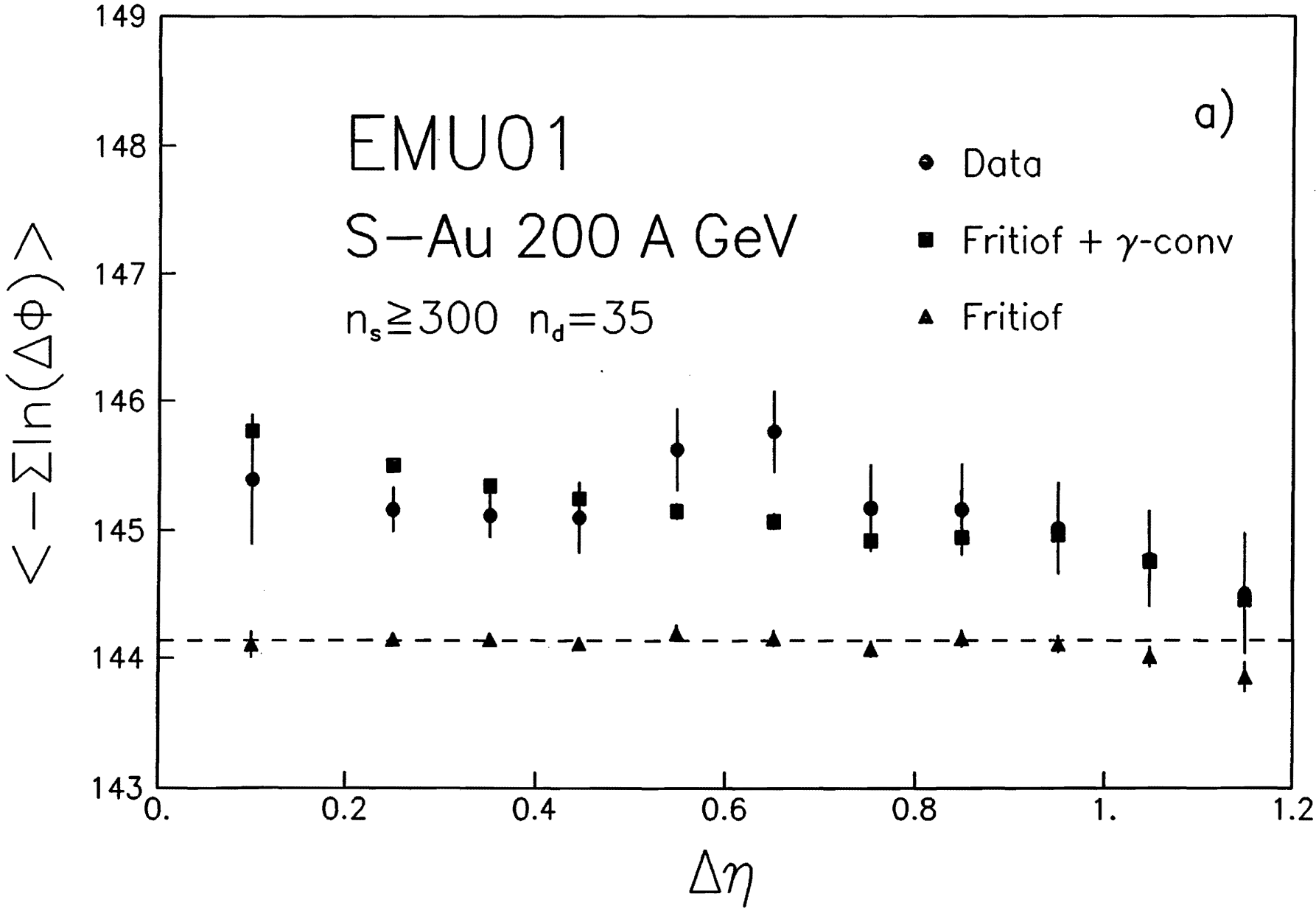
EMU01
S–Au 200 A GeV
$n_s \geq 300$ $n_d = 35$
a)
Data
Fritiof + γ-conv
Fritiof
$\langle -\sum \ln(\Delta\phi) \rangle$
$\Delta\eta$
149
148
147
146
145
144
143
0.
0.2
0.4
0.6
0.8
1.
1.2

Fig. 4

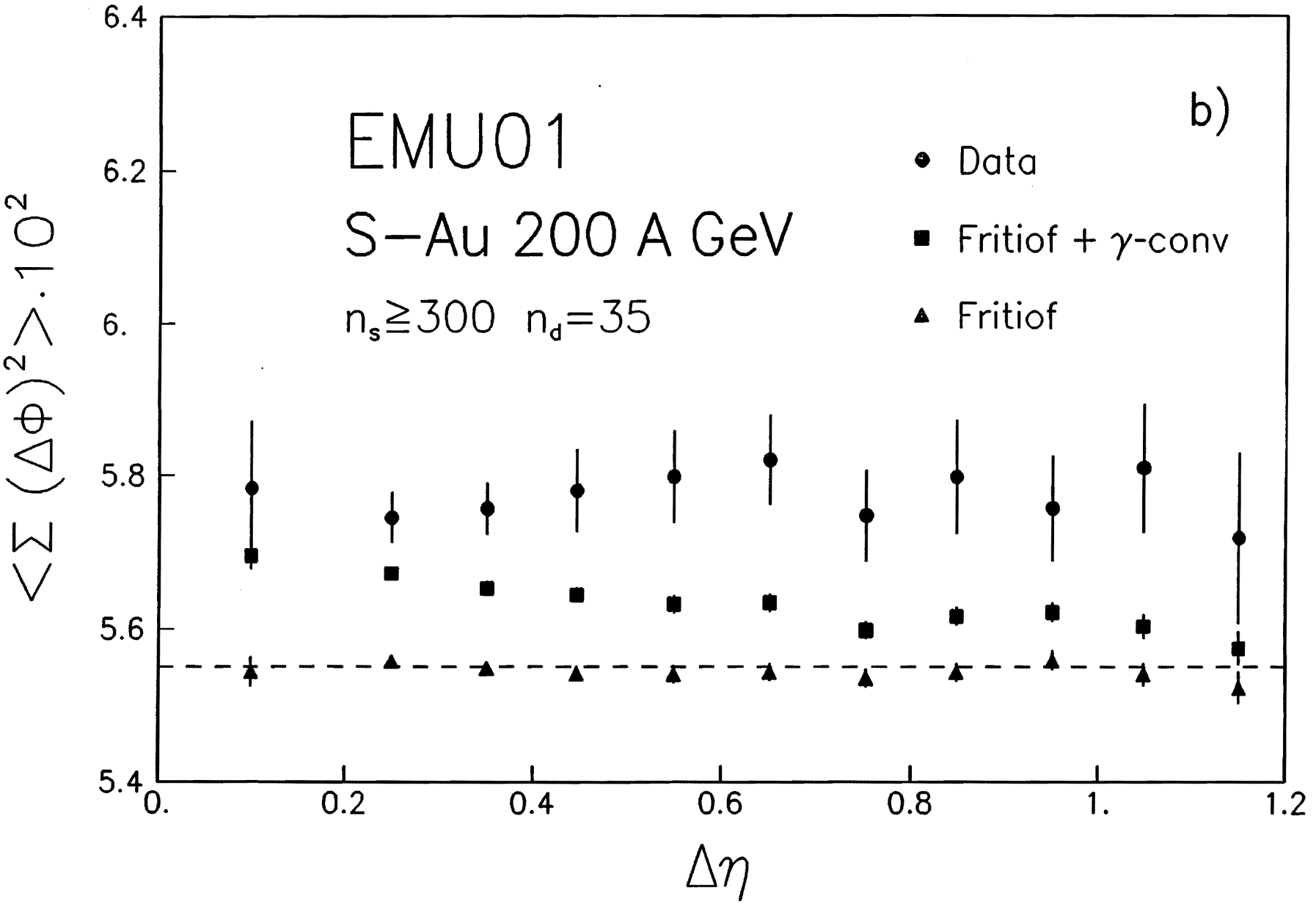
EMU01
S–Au 200 A GeV
$n_s \geq 300$ $n_d = 35$
b)
Data
Fritiof + γ-conv
Fritiof
$\langle \sum (\Delta\phi)^2 \rangle \cdot 10^2$
$\Delta\eta$
6.4
6.2
6.
5.8
5.6
5.4
0.
0.2
0.4
0.6
0.8
1.
1.2

Fig. 4

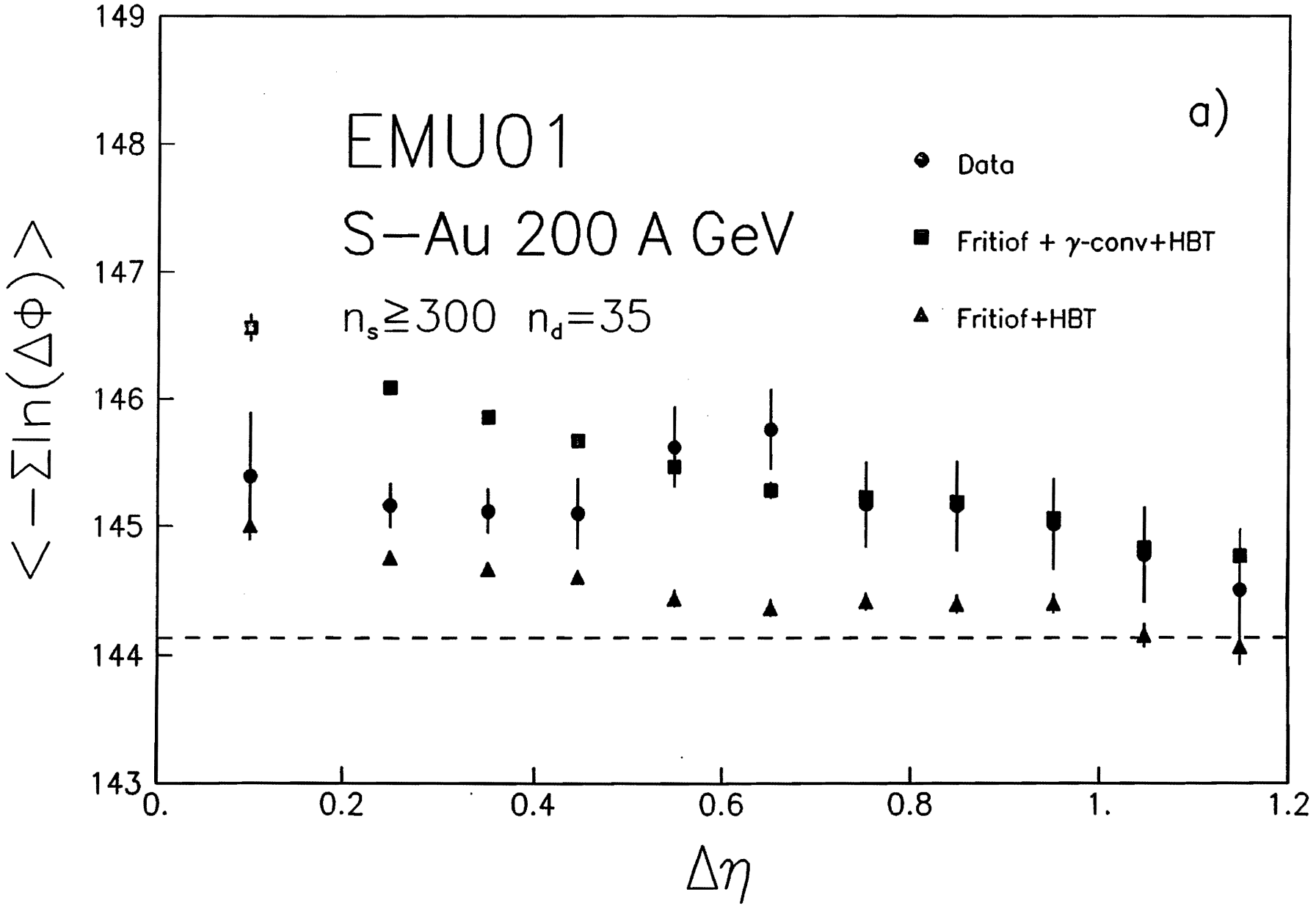
EMU01
S−Au 200 A GeV
$n_s \geq 300$ $n_d = 35$
a)
Data
Fritiof + γ-conv+HBT
Fritiof+HBT
$\langle -\sum \ln(\Delta\phi) \rangle$
$\Delta\eta$
149
148
147
146
145
144
143
0.
0.2
0.4
0.6
0.8
1.
1.2

Fig. 5

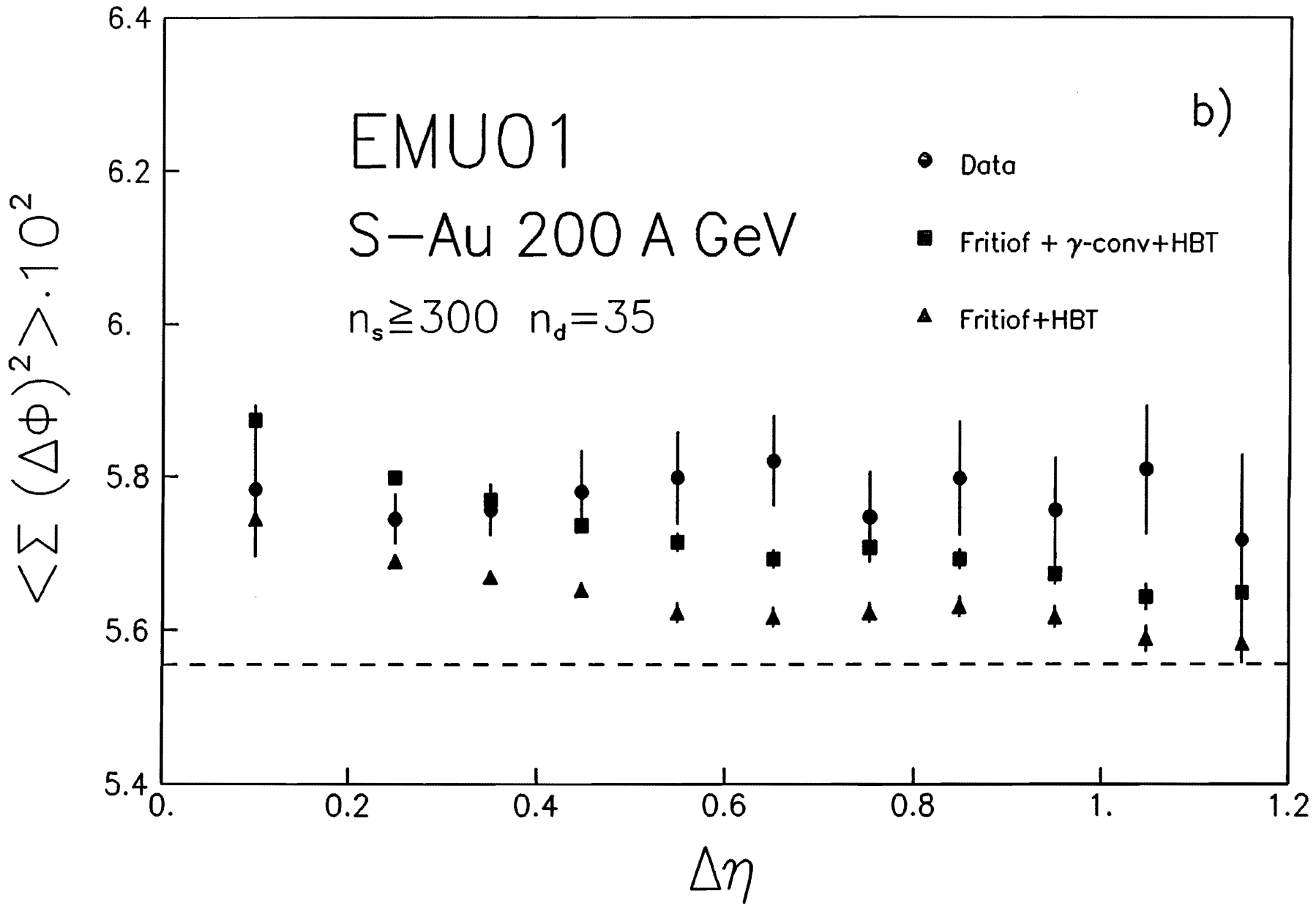
EMU01
S–Au 200 A GeV
$n_s \geq 300$ $n_d = 35$
b)
Data
Fritiof + γ-conv+HBT
Fritiof+HBT
$\langle \sum (\Delta\phi)^2 \rangle \cdot 10^2$
$\Delta\eta$
6.4
6.2
6.
5.8
5.6
5.4
0.
0.2
0.4
0.6
0.8
1.
1.2

Fig. 5

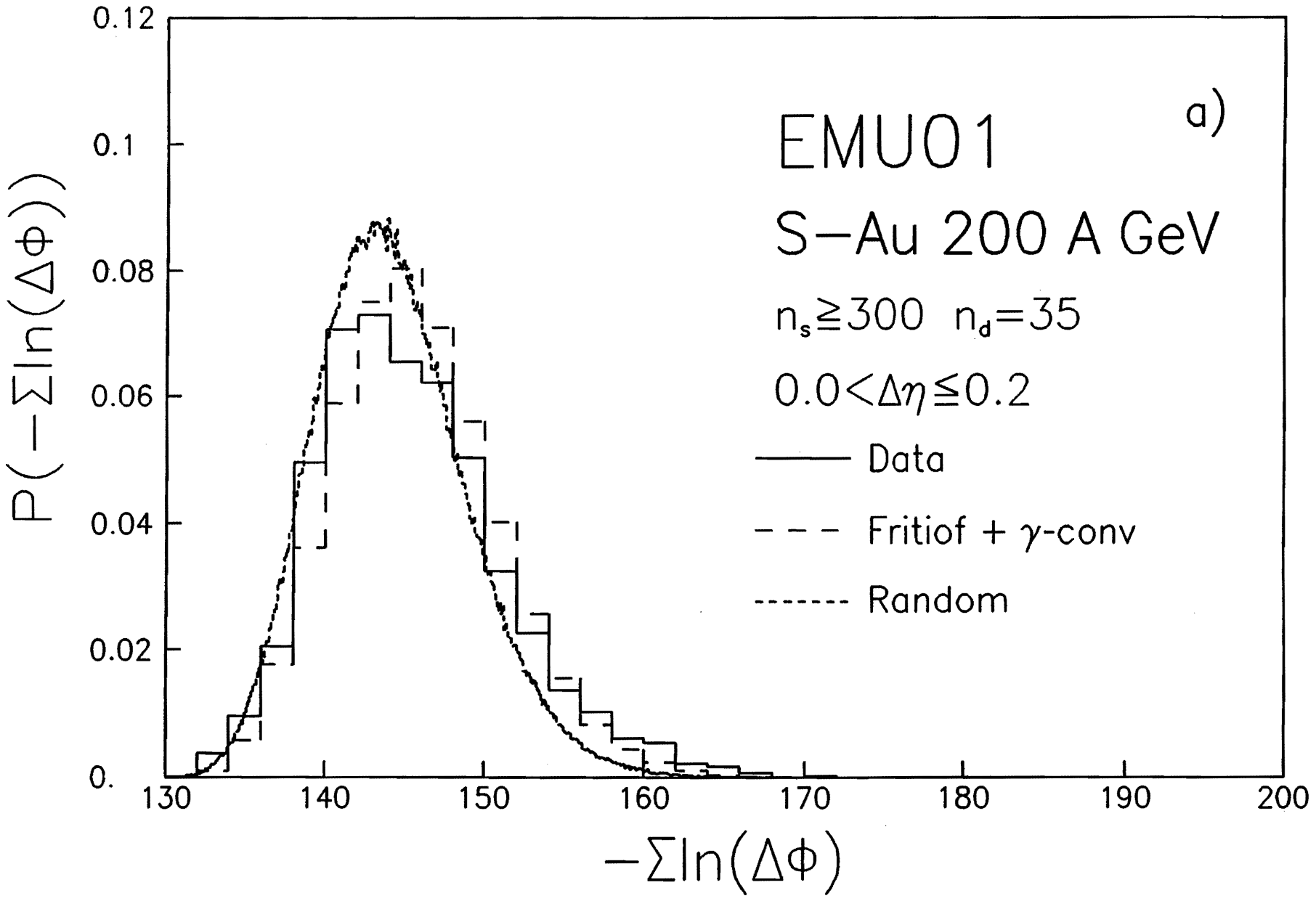
EMU01
a)
S−Au 200 A GeV
$n_s \geq 300$ $n_d = 35$
$0.0 < \Delta\eta \leq 0.2$
Data
Fritiof + γ-conv
Random
$P(-\Sigma \ln(\Delta\phi))$
$-\Sigma \ln(\Delta\phi)$
0.12
0.1
0.08
0.06
0.04
0.02
0.
130
140
150
160
170
180
190
200

Fig. 6

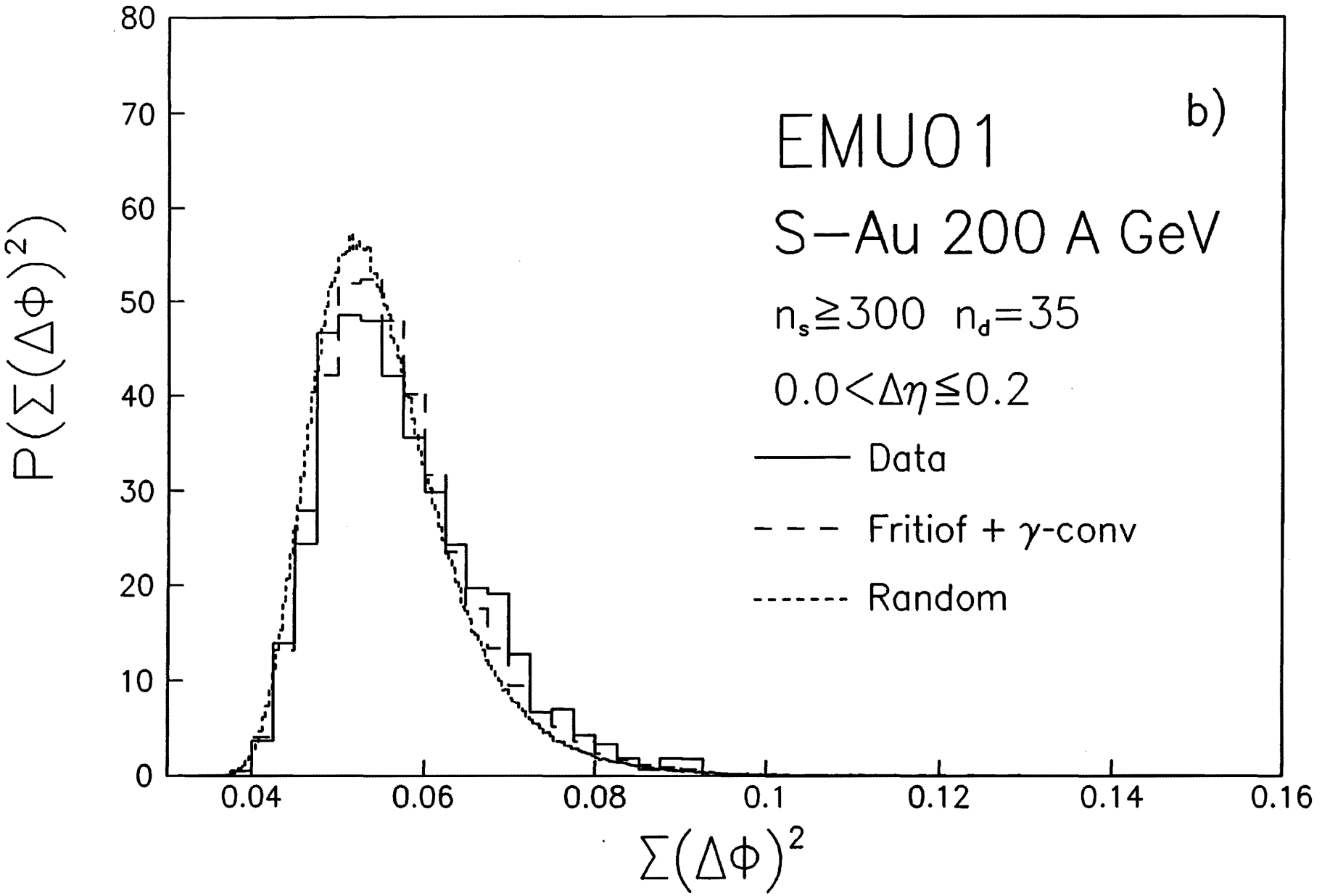
EMU01
b)
S−Au 200 A GeV
$n_s \geq 300$ $n_d = 35$
$0.0 < \Delta\eta \leq 0.2$
Data
Fritiof + γ-conv
Random
$P(\Sigma(\Delta\phi)^2)$
$\Sigma(\Delta\phi)^2$
0
10
20
30
40
50
60
70
80
0.04
0.06
0.08
0.1
0.12
0.14
0.16

Fig. 6

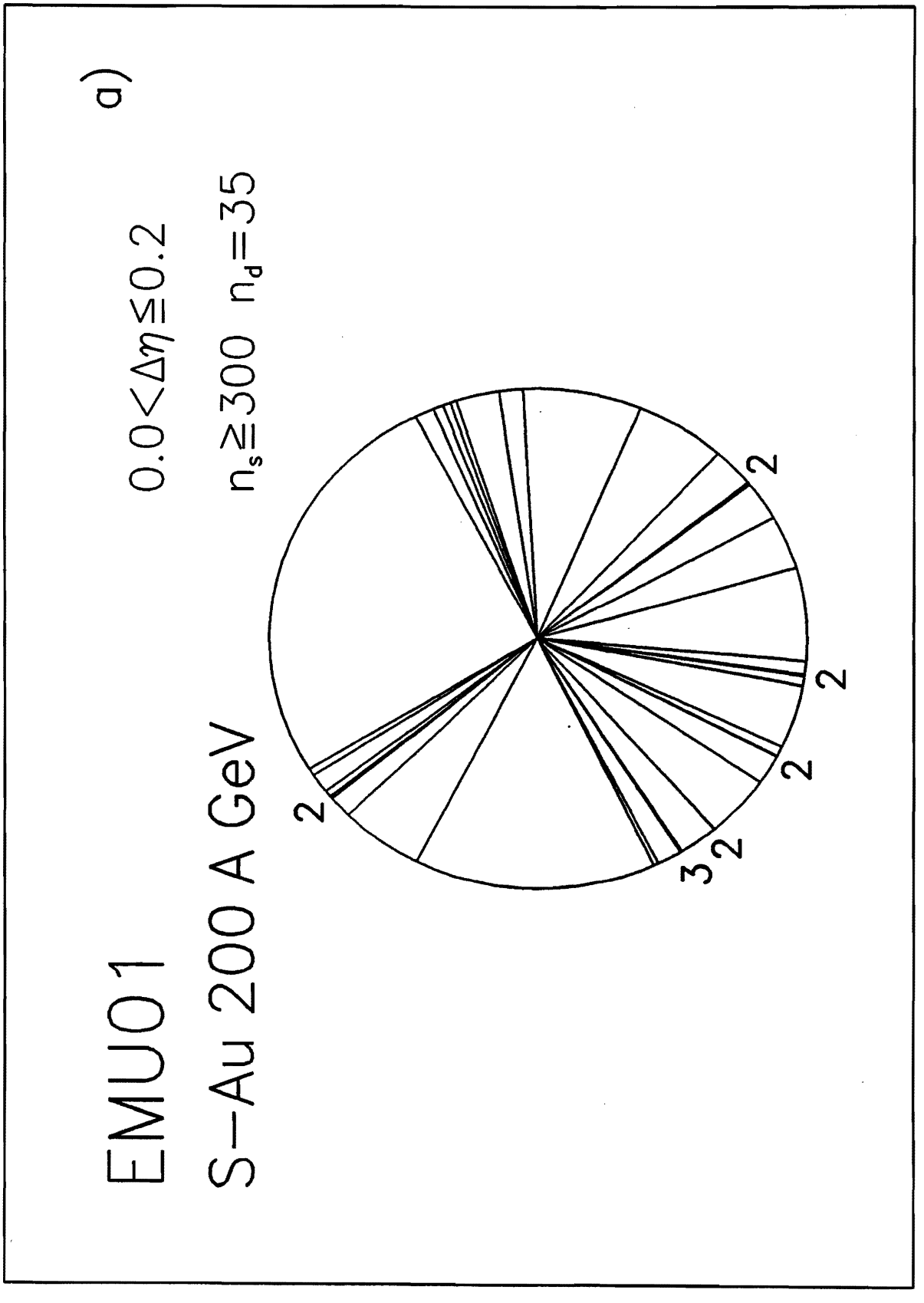

Fig. 7

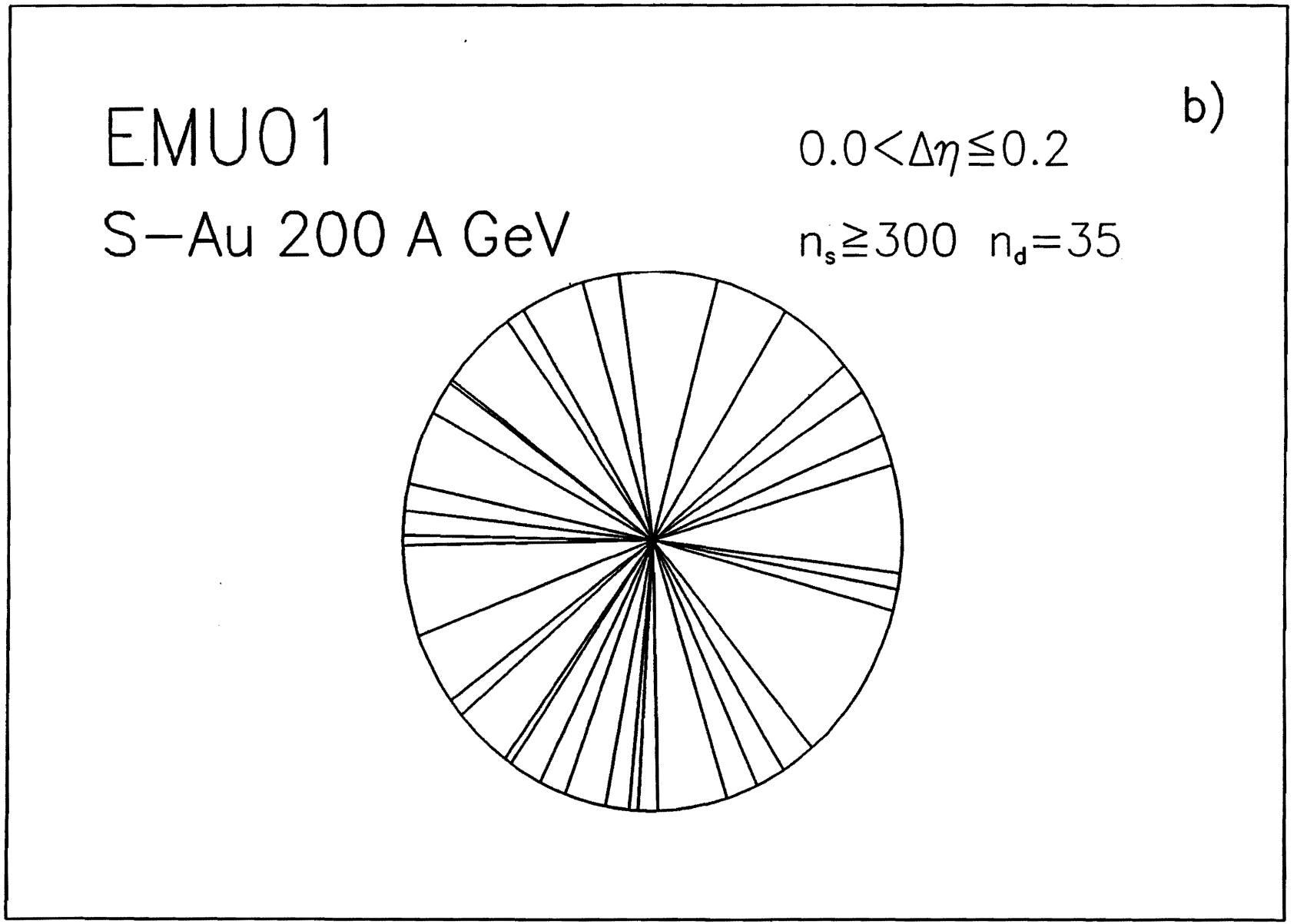

Fig. 7

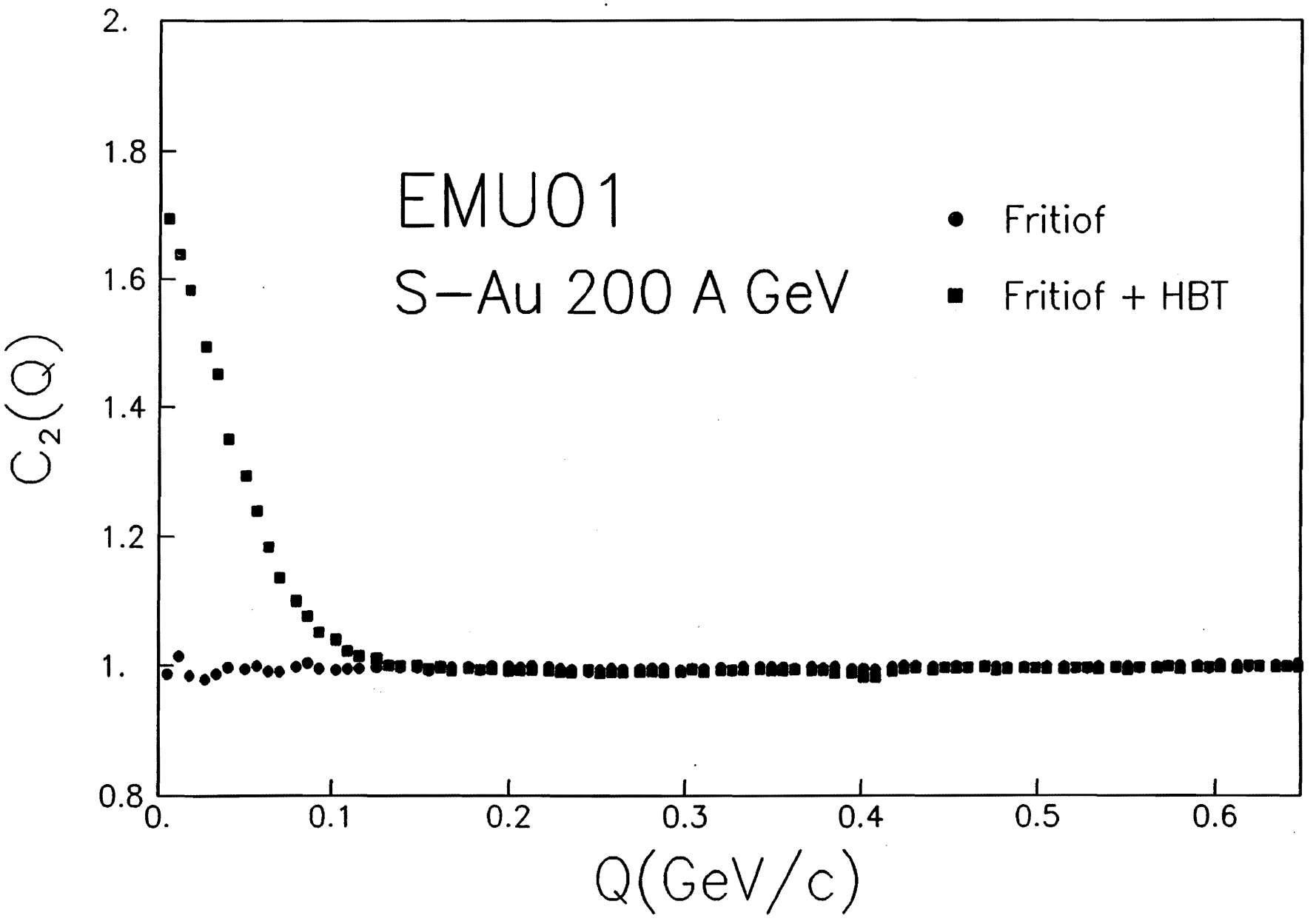
EMU01
S–Au 200 A GeV
Fritiof
Fritiof + HBT
$C_2(Q)$
Q(GeV/c)
2.
1.8
1.6
1.4
1.2
1.
0.8
0.
0.1
0.2
0.3
0.4
0.5
0.6

Fig. 8